

Article

Trivalent Cobalt Complexes with NNS Tridentate Thiosemicarbazones: Preparation, Structural Study and Investigation of Antibacterial Activity and Cytotoxicity against Human Breast Cancer Cells

Amany Fathy ¹, Ahmed B. M. Ibrahim ^{2,*} , S. Abd Elkhaliq ¹, Alexander Villinger ³  and S. M. Abbas ¹ ¹ Chemistry Department, Faculty of Science, Beni-Suef University, Beni-Suef 62521, Egypt² Department of Chemistry, Faculty of Science, Assiut University, Assiut 71516, Egypt³ Institut für Chemie, Universität Rostock, Albert-Einstein-Str. 3a, 18059 Rostock, Germany

* Correspondence: aibrahim@aun.edu.eg



Citation: Fathy, A.; Ibrahim, A.B.M.; Abd Elkhaliq, S.; Villinger, A.; Abbas, S.M. Trivalent Cobalt Complexes with NNS Tridentate Thiosemicarbazones: Preparation, Structural Study and Investigation of Antibacterial Activity and Cytotoxicity against Human Breast Cancer Cells. *Inorganics* **2022**, *10*, 145. <https://doi.org/10.3390/inorganics10090145>

Academic Editors: Duncan H. Gregory, Torben R. Jensen, Claudio Pettinari, Vladimir Arion, Wolfgang Linert and Richard Dronskowski

Received: 18 July 2022

Accepted: 14 September 2022

Published: 19 September 2022

Publisher's Note: MDPI stays neutral with regard to jurisdictional claims in published maps and institutional affiliations.



Copyright: © 2022 by the authors. Licensee MDPI, Basel, Switzerland. This article is an open access article distributed under the terms and conditions of the Creative Commons Attribution (CC BY) license (<https://creativecommons.org/licenses/by/4.0/>).

Abstract: New complexes of trivalent cobalt with substituted thiosemicarbazone ligands having an NNS donor system {**HL**¹ = 4-(4-nitrophenyl)-1-((pyridin-2-yl)methylene)thiosemicarbazide and **HL**² = 4-(2,5-dimethoxyphenyl)-1-((pyridin-2-yl)methylene)thiosemicarbazide} were synthesized via the in situ oxidation of divalent cobalt chloride accompanying its addition to the ligands. The complexes **C1** and **C2** were characterized via elemental (CHNS) analysis and ¹H NMR, FT-IR and UV-Vis. spectroscopic data. Further, conductometric studies on the DMF solutions of the complexes indicated their 1:1 nature, and their diamagnetism revealed the low-spin trivalent oxidation state of the cobalt in the complexes. The X-ray diffraction analysis of complex **C1** indicated that it crystallizes in the triclinic space group P-1. The metal exhibits an octahedral environment built by two anionic ligands bound via pyridine nitrogen, imine nitrogen and thiol sulfur atoms. The complex is counterbalanced by a chloride ion. In addition, two lattice water molecules were detected in the asymmetric unit of the unit cell. The ligand **HL**² (20 mg/mL in DMSO) displayed inhibition zones of 10 mm against both *S. aureus* and *E. coli*, and the same concentration of the respective complex raised this activity to 15 and 12 mm against these bacterial strains, respectively. As a comparison, ampicillin inhibited these bacterial strains by 21 and 25 mm, respectively. Screening assay by **HL**¹ on four human cancer cells revealed the most enhanced activity against the breast MCF-7 cells. The induced growth inhibitions in the MCF-7 cells by all compounds (0–100 µg/mL) have been detected. The ligands (**HL**¹ and **HL**²) and complex **C2** gave inhibitions with IC₅₀ values of 52.4, 145.4 and 49.9 µM, respectively. These results are more meaningful in comparison with similar cobalt complexes, but less efficient compared with the inhibition with IC₅₀ of 9.66 µM afforded by doxorubicin. In addition, doxorubicin, **HL**¹ and **HL**² induced cytotoxicity towards healthy BHK cells with IC₅₀ values of 36.42, 54.8 and 110.6 µM, but surviving fractions of 66.1% and 62.7% of these cells were detected corresponding to a concentration of 100 µg/mL of the complexes (136.8 µM of **C1** and 131.4 µM of **C2**).

Keywords: monoanionic ligands; tridentate NNS ligands; diamagnetism; X-ray crystal structure; anticancer activity; antibacterial activity

1. Introduction

Cobalt is an essential element for maintaining good human health, its role being predominately associated with the function of cobalamin (vitamin B12) that indirectly regulates growth and the DNA synthesis, in addition to its role in creating red blood cells and maintaining a healthy nervous system [1]. Compared with other metal compounds, the cobalt ones as pharmaceuticals have been much less explored in the literature [2–10]. Nevertheless, the cobalt compounds are seen as imaging agents [2], hypoxia-targeting

agents [3], enzyme inhibitors [4] and drug-delivery scaffolds [5]. This is in addition to their functions as anticancer [6], antiviral [7], antifungal [8] and antibacterial [9] agents. Doxovir, for instance, is a common Schiff base complex of a trivalent cobalt cation acting as a therapeutic in clinical trials and showing efficiency, in a vague mechanism, against the herpes simplex virus 1 (HSV1) [7]. A unique property of trivalent cobalt compared with other 3d metal ions that grants its usefulness in medicine is that the trivalent cobalt complexes are kinetically inert due to the cobalt(III) low-spin d^6 electron configuration [10]. This permits ligand substitution reactions in Co(III) complexes, compared with divalent cobalt complexes, on much slower rates [10]. This dichotomy between divalent and trivalent cobalt ions allows for the development of trivalent cobalt prodrugs that become reduced in the biological systems to form labile divalent cobalt complexes (d^7 complexes) that afterwards release their ligands, leading to cell cytotoxicity [11]. This reductive release strategy has been investigated for several classes of Co(III) complexes, with the ultimate objective being the selective targeting of the hypoxic environments [3].

Thiosemicarbazones (TSCs) are a class of Schiff base N and S donor ligands formed via the condensation of thiosemicarbazides with various carbonyl compounds [12–15]. The TSC ligands can react with the metals as neutral or monoanionic species; crystallography can determine these different binding modes, as the C–S bond in the neutral form is a double bond of 1.67–1.72 Å, while the deprotonated TSC form produces a formal C–S single bond of 1.71–1.80 Å [16]. The interest in the TSCs is driven by a potential significance in their biological applicability, due to their ability for DNA binding [17,18], as anticancer [19–21], bactericidal [22], fungicidal [23,24], antitrypanosomal [25,26] and antimalarial [27] agents. In general, the heterocyclic TSCs were reported to give more valuable biological activities compared with the aromatic ones; triapine (3-aminopyridine-2-carboxaldehyde thiosemicarbazone), an example of N(4)-substituted TSCs, has been involved in a phase I trial for patients suffering from advanced solid tumors [12–15]. The mechanism of action of the TSCs in medicine is still controversial, but it was concluded that these compounds act via inhibiting the enzyme ribonucleotide reductase that affects the biosynthesis of DNA precursors [12,13].

In view of this introduction, this paper presents the preparation of two trivalent cobalt complexes, acronymed as **C1** and **C2**, produced via the reactions of cobalt(II) chloride hexahydrate with the tridentate thiosemicarbazone ligands {**HL**¹ = 4-(4-nitrophenyl)-1-((pyridin-2-yl)methylene)thiosemicarbazide and **HL**² = 4-(2,5-dimethoxyphenyl)-1-((pyridin-2-yl)methylene)thiosemicarbazide}. Following the synthesis and full characterization of these cobalt complexes, we here report the antibacterial activities of these complexes and their ligands against a Gram +ve (*S. aureus*) and a Gram –ve (*E. coli*) bacterial species, in addition to the cytotoxic behavior of these compounds against human breast cancer MCF-7 cells.

2. Results and Discussion

2.1. Formation of the Cobalt(III) Complexes

Detailed information on the synthesis of **HL**¹ [28] and **HL**² [29] (Figure 1) was described in the respective literature. Briefly, the reaction of 4-nitrophenyl isothiocyanate for **HL**¹ or 2,5-dimethoxyphenyl isothiocyanate for **HL**² with hydrazine hydrate produced thiosemicarbazides. These thiosemicarbazides were filtered, acidified in ethanolic solutions with droplets of glacial acetic acid and reacted with 2-formylpyridine to obtain the Schiff base ligands. The crystallization of the ligands with aqueous ethanol resulted in pure products analyzed by elemental microanalysis and spectroscopic techniques (¹H-NMR, ¹³C-NMR, UV-Visible and FT-IR). As solutions in DMSO-*d*₆, the proton (Figure 2) and ¹³C NMR (Figure 3) spectra of **HL**¹ and **HL**² were determined. The ¹HMR spectrum of **HL**¹ cleared three singlet resonances integrated for the hydrazine NH (8.62 ppm), thiourea NH (10.48 ppm) and azomethine CH (12.27 ppm) protons. This is in addition to the appearance of multiple peaks {doublet and triplet} in the range of 7.43–8.40 ppm assigned to the pyridine and benzene ring protons. On another hand, the proton NMR spectrum of **HL**²

showed the same singlet peaks of **HL**¹ at 8.21, 10.10 and 12.16 ppm, in addition to a sum of seven peaks (two triplet, four doublet and one singlet) in the 6.75–8.61 ppm range due to the ring protons. Furthermore, two singlet resonances at 3.72 and 3.85 ppm due to the two methoxy groups' protons were observed in the spectrum of **HL**². The ¹³C NMR spectrum of **HL**¹ showed peaks at 116.88, 120.95, 123.43, 123.78, 124.70, 136.51, 143.85, 144.29, 144.79, 149.23, 152.47 and 175.78 ppm, and that of **HL**² showed peaks at 55.01, 56.08, 109.04, 109.92, 112.11, 119.09, 123.86, 128.01, 136.28, 142.61, 145.42, 149.17, 152.12, 152.43 and 174.89 ppm. In general, rather than the chemical shifts at 55.01 and 56.08 ppm corresponding to the two methoxy groups in **HL**², the other ligand peaks are located at almost-similar positions, indicating similar structures of the ligands. The exhibition of this ligand class of solution thione-thiol tautomerism and their act in a monoanionic manner upon chelation in their complexes were reported [30–34].

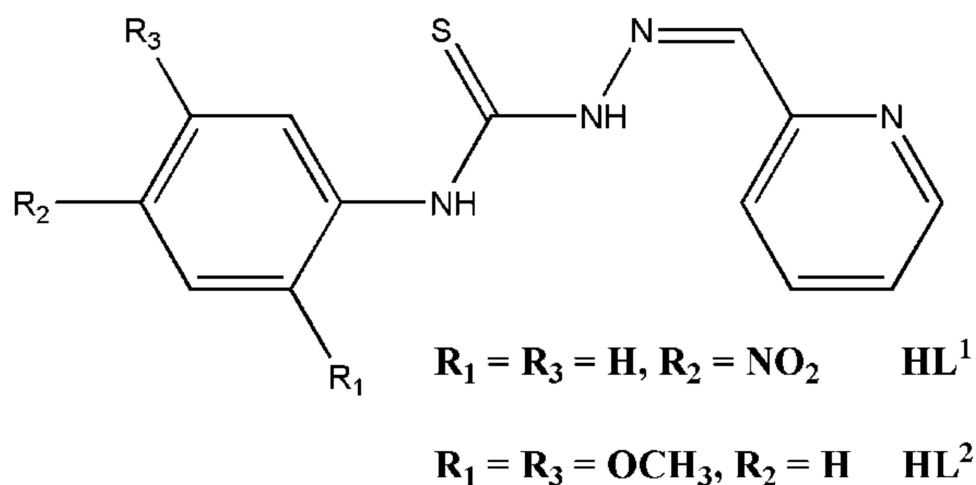


Figure 1. Structures of the TSC ligands.

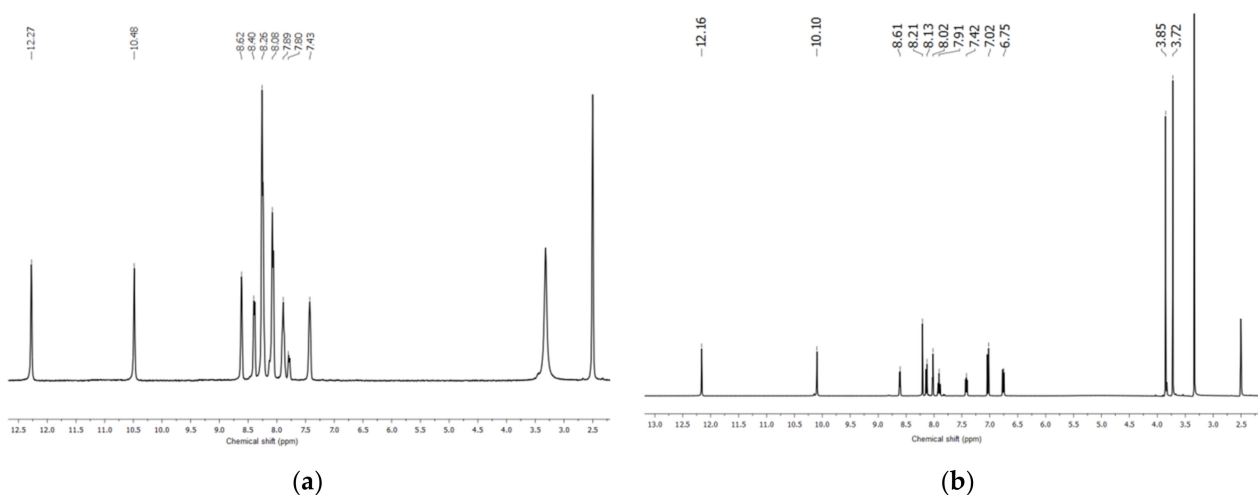


Figure 2. ¹H NMR spectra of **HL**¹ (a) and **HL**² (b) measured in DMSO-d₆.

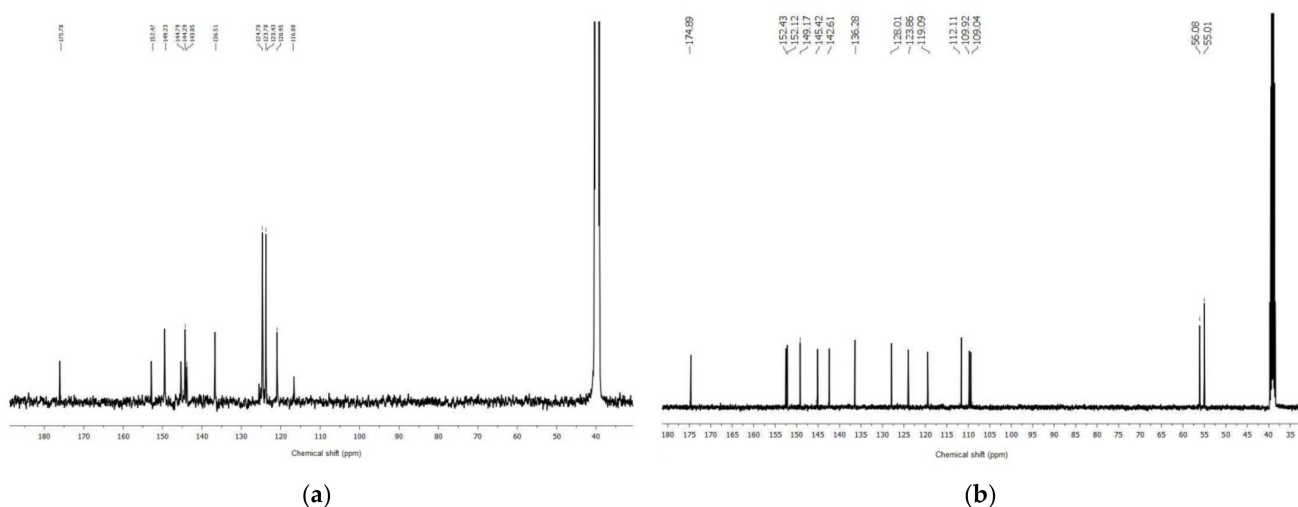


Figure 3. ^{13}C NMR spectra of **HL**¹ (a) and **HL**² (b) measured in DMSO-d_6 .

The reactions between 1:2 molar amounts of cobalt(II) chloride hexahydrate and the TSC ligands occurred in methanol. Although the ligand solutions turned dark immediately after the addition of the cobalt(II) chloride, indicating the formation of cobalt complexes, these complexes required a relatively long time to separate out in the solid form (around one month). The complexes **C1** and **C2** formed in moderate yields (67% for **C1** and 59% for **C2**). These complexes showed very good solubility in a wide variety of organic solvents, including acetone, acetonitrile, chlorinated hydrocarbons (dichloromethane and chloroform) and alcohols (methanol and ethanol). Preliminary analyses of these complexes by the measuring of their CHNS contents, magnetic susceptibilities and electrical conductivities in DMF solutions (1 mM) were conducted. The elemental data revealed the combination of two ligand anions, a chloride ion and two water molecules with the cobalt cation in the complexes. The magnetic susceptibilities were almost zero, assigning diamagnetism to the complexes. The molar conductivity values of complexes **C1** and **C2** were of $72.12\text{--}77.81 \Omega^{-1}\text{cm}^2\text{mol}^{-1}$ in the range reported for 1:1 electrolytes [35,36], and these values did not markedly change after 24 h of clearing the complexes' stability in their solutions [36].

The diamagnetism of **C1** and **C2** indicates the rapid oxidation of the cobalt(II) cation, once bound to the TSC ligand, to its trivalent form. In general, Co(II) is a stable high-spin cation of pink color in both water and methanol. This cobalt(II) cation has a $t_{2g}^5e_g^2$ electron configuration. In addition to a strong field ligand, the cation electrons attain the low spin state $t_{2g}^6e_g^1$. Indeed, the ligands sometimes have a strong enough field (e.g., TSC ligands) to cause great splitting between these energy states. This leads to the oxidation of the Co(II) cation to the trivalent oxidation state due to the destabilization of the single electron in the cobalt(II) cation and its removal [37].

The isolated complexes were further characterized by spectroscopic (^1H NMR, FT-IR and UV-Visible) analyses. The ^1H NMR spectra of the complexes (Figure 4) are similar to the ligands', but the disappearance of the singlet peaks of the hydrazine hydrogen indicates the coordination in the thiol form. On the other hand, the ^{13}C NMR spectra (Figure 5) exhibits only five and eight peaks for complexes **C1** and **C2**, respectively. The compounds **HL**¹ (30 mg), **HL**² (32 mg), **C1** (73 mg) and **C2** (76 mg) were dissolved in dichloromethane to form 10 mL of a stock solution of 10 mM of each compound. The successive dilution of these solutions was performed thrice that in each step 1 mL of each solution was diluted with dichloromethane (total volume = 10 mL). The final solutions of 10 μM were then used in the UV-visible spectral measurements. The spectrum of each ligand (Figure 6) displayed only an absorption at 333 nm for **HL**¹ and 326 nm for **HL**² both assigned for intraligand $n\text{-}\pi^*$ transitions [36]. The spectra of complexes **C1** and **C2** are very dissimilar to the ligands'. Complex **C1** displays two distinct absorption maxima at 384 and 239 nm, while complex

C2 displays three peaks at 255 (sh), 296 and 428 nm. The peaks recorded at 239, 255 and 296 nm are intraligand-based [36], but the electronic transitions at 384 and 428 nm are due to ligand-to-metal charge transfer [36]. Indeed, Co(III) complexes with octahedral symmetry should give bands due to $^1A_{1g} \rightarrow ^1T_{1g}$, $^1A_{1g} \rightarrow ^1T_{2g}$, $^1A_{1g} \rightarrow ^3T_{1g}$ and $^1A_{1g} \rightarrow ^3T_{2g}$ transitions [38]. However, the identification of these d-d bands is complicated by overlap with the charge transfer bands and the presence of weak spin-forbidden transition bands [38].

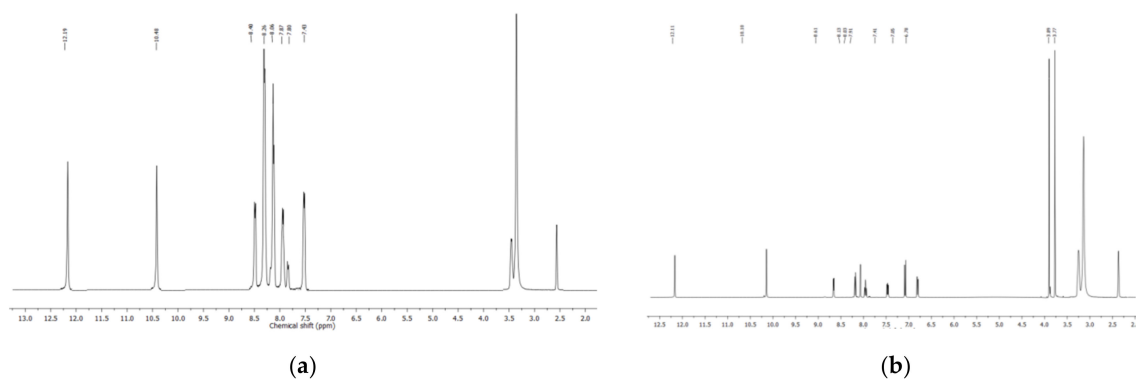


Figure 4. ^1H NMR spectra of **C1** (a) and **C2** (b) measured in DMSO-d_6 .

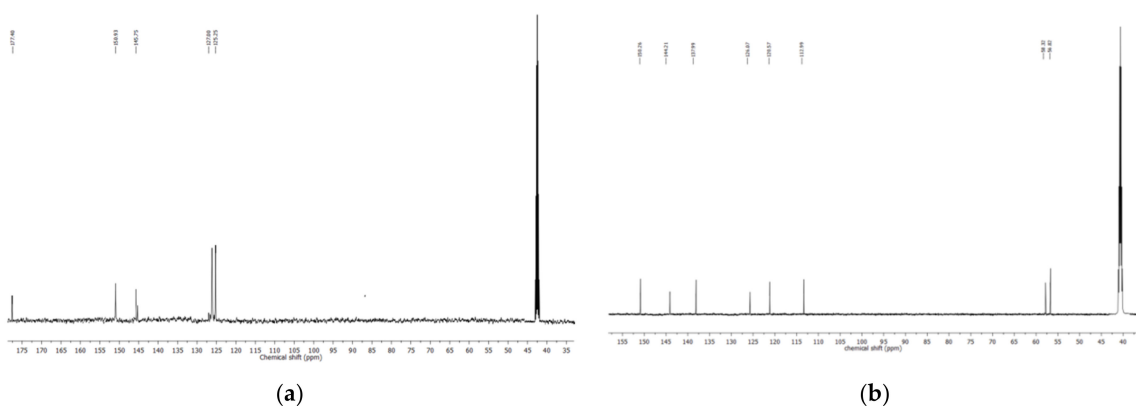


Figure 5. ^{13}C NMR spectra of **C1** (a) and **C2** (b) measured in DMSO-d_6 .

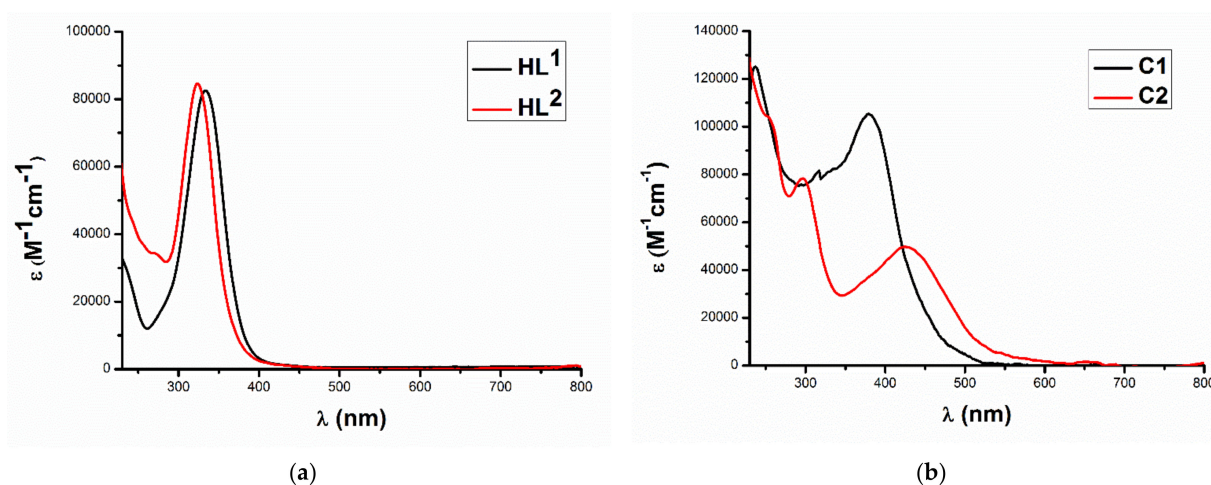


Figure 6. UV-Visible spectra of compounds $\{\text{HL}^1$ and $\text{HL}^2\}$ (a) and compounds $\{\text{C1}$ and $\text{C2}\}$ (b) measured in dichloromethane.

With respect to the FT-IR spectral data measured for the compounds in KBr pellets, the exhibition of bands at 3116 cm^{-1} for **HL**¹ and 3136 cm^{-1} for **HL**² is attributed to $\nu(^2\text{NH})$ vibrations. The disappearance of these transitions in the spectra of complexes **C1** and **C2** reveals the deprotonation of these ligands in the complexes [32]. The bands for vibrations of the thioamide moiety $\{\nu(\text{CS}) + \nu(\text{CN})\}$, seen at 1330 and 846 cm^{-1} in the **HL**¹ spectrum and at 1391 and 842 cm^{-1} in the **HL**² spectrum, underwent movement to 1312 and 791 cm^{-1} in the complex **C1** spectrum and to 1314 and 819 cm^{-1} in that of the complex **C2**. These results indicate existence of bonding with the TSC sulfur in both of the complexes [33]. The TSC $^4\text{N}-\text{H}$ moiety is known to involve in hydrogen bonds of various strengths before and after the metal coordination; this shifts the respective stretching bands of the ligands to higher wavenumbers in the spectra of the complexes [32]. Each ligand spectrum exhibited a band attributed to stretching vibrations in the ligand azomethine bonds (at 1582 cm^{-1} for **HL**¹ and 1606 cm^{-1} for **HL**²), the cobalt coordination affected these bands to place at lower wavenumbers in the range of 1523 – 1572 cm^{-1} in the complexes' spectra [33]. The indicated azomethine-cobalt coordination in the complexes can also be proven by new bands at 589 – 578 cm^{-1} for $\nu(\text{Co}-\text{N}_{\text{azomethine}})$ in their spectra [33]. The stretching vibrational transitions of the ligand $\text{N}-\text{N}$ bonds are found in the 1051 – 1078 cm^{-1} range in their spectra; however, these bands blueshifted to the wavenumber 1098 – 1099 cm^{-1} range in the spectra of **C1** and **C2** [34]. The cobalt coordination with the TSC pyridine rings is indicated by bands in the ranges of 644 – 688 cm^{-1} and 427 – 452 cm^{-1} assigned for both of in-plane and out-of-the-plane pyridine ring deformation. However, these bands locate at 664 and 404 cm^{-1} for **HL**¹ and at 622 and 407 cm^{-1} for **HL**² in the spectra of the free ligands [30].

2.2. X-ray Diffraction Analysis

Table 1 gives a summary of the crystal structure and the refinement data for complex **C1**. The selected bond lengths and angles in the complex are provided in Table 2. As presented in Figure 7 (molecular structure of the complex), the crystallographic asymmetric unit of the complex contains a mononuclear complex cation composed of two identical N_2S tridentate anionic ligands both wrapped around a cobalt(III) ion exhibiting a six coordination geometry. In the asymmetric unit, a chloride anion (Cl1) and two water molecules (O5, O6) of crystallization (one of them is disordered over two positions) were also found.

Table 1. Crystallographic data for the cobalt(III) complex **C1**.

Empirical formula	$\text{C}_{26}\text{H}_{24}\text{N}_{10}\text{O}_6\text{S}_2\text{CoCl}$	μ (mm^{-1})	0.872
Formula weight	731.05	F (000)	748.0
Crystal system	Triclinic	θ range for data collection ($^\circ$)	2.508 to 25.499
space group	P -1	Reflections collected	5446
a (\AA)	11.8902 (8)	Unique refl. collected (R_{int})	4012 (0.0536)
b (\AA)	12.4093 (8)	Completeness to theta	98.9%
c (\AA)	12.5613 (9)	Parameters (Restraints)	511(537)
α ($^\circ$)	118.026 (2)	Max. and min. transmission	0.746 and 0.665
β ($^\circ$)	108.500 (2)	GOF on F^2	1.090
γ ($^\circ$)	95.735 (2)	$R1$ [$I > 2\sigma(I)$]	0.0581
Volume (\AA^3)	1481.28 (18)	wR2 (all data)	0.1582
Z	2	Largest diff. peak, hole/ $e\text{\AA}^{-3}$	0.838 and -0.483
Density (g/cm^3)	1.639	CCDC number	2175750

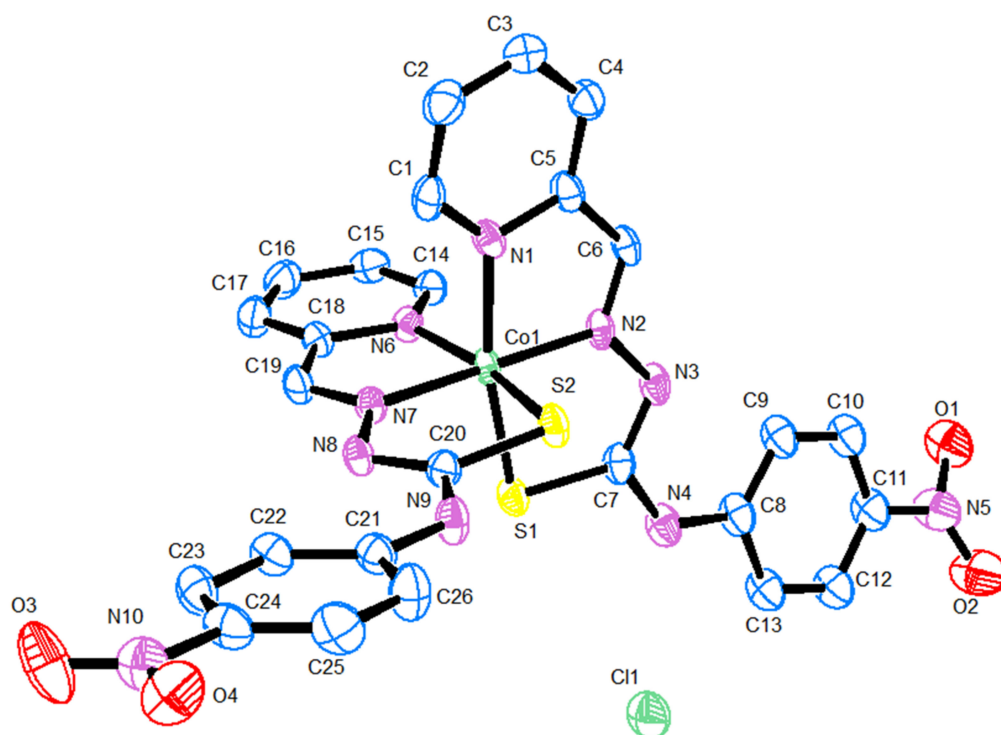


Figure 7. Molecular drawing of $[\text{Co}(\text{L}^1)_2]\text{Cl}\cdot 2\text{H}_2\text{O}$ (C1) with thermal ellipsoids at 50% probability level (the crystallization water molecules and all H atoms have been removed for more clarity).

Table 2. Selected bond lengths (Å) and angles ($^\circ$) for complex C1.

Atoms	Distance (Å)	Atoms	Angle ($^\circ$)	Atoms	Angle ($^\circ$)
Co1—S1	2.215 (1)	S1—Co1—S2	90.50 (5)	Co1—S2—C20	94.4 (2)
Co1—S2	2.208 (2)	S1—Co1—N1	168.0 (1)	Co1—N1—C1	129.1 (3)
Co1—N1	1.969 (3)	S1—Co1—N2	85.1 (1)	Co1—N1—C5	111.2 (3)
Co1—N2	1.885 (4)	S1—Co1—N6	91.4 (1)	Co1—N2—N3	124.8 (3)
Co1—N6	1.971 (5)	S1—Co1—N7	95.3 (1)	Co1—N2—C6	116.1 (3)
Co1—N7	1.881 (4)	S2—Co1—N1	89.9 (1)	Co1—N6—C14	129.9 (3)
S1—C7	1.741 (6)	S2—Co1—N2	93.3 (1)	Co1—N6—C18	111.8 (3)
S2—C20	1.744 (5)	S2—Co1—N6	168.1 (1)	Co1—N7—N8	124.3 (3)
N1—C1	1.317 (6)	S2—Co1—N7	85.8 (1)	Co1—N7—C19	117.0 (3)
N1—C5	1.366 (6)	N1—Co1—N2	82.9 (2)	C1—N1—C5	119.5 (4)
N2—N3	1.362 (5)	N1—Co1—N6	90.7 (2)	N3—N2—C6	119.1 (4)
N2—C6	1.297 (4)	N1—Co1—N7	96.7 (2)	N8—N7—C19	118.7 (4)
N6—C14	1.331 (6)	N2—Co1—N6	98.6 (2)	C14—N6—C18	118.3 (4)
N6—C18	1.368 (7)	N2—Co1—N7	179.1 (2)	N2—N3—C7	111.0 (4)
N7—N8	1.377 (5)	N6—Co1—N7	82.3 (2)	N7—N8—C20	110.7 (4)
N7—C19	1.285 (8)	Co1—S1—C7	94.6 (2)		

The coordination is realized via imine nitrogen (N2, N7), thiolate sulfur (S1, S2) and pyridine nitrogen (N1, N6) atoms, with the formation of four 5-membered chelate rings in the complex (Figure 7). The donor atoms around the cobalt(III) cation form a distorted octahedron with the ligands having almost coplanar atoms meridionally coordinated, so that the imine nitrogen atoms (N2 and N7) are *trans*-located with a N2—Co1—N7 bond angle of 179.1 (2) $^\circ$. On the other hand, the pyridine nitrogen atoms (N1 and N6) and the sulfur atoms (S1 and S2) are in *cis*-positions, with bite angles of 90.7 (2) $^\circ$ [N1—Co1—N6] and of 90.50 (5) $^\circ$ [S1—Co1—S2]. The donor atoms in each ligand anion are almost coplanar, and the two NNS planes are orthogonal to each other. The Co—S bond distances are of 2.215 (1)–2.208 (2) Å, and the Co—N distances fall in the range 1.881 (4)–1.971 (5) Å.

However, the Co—N(pyridine) bonds {1.969 (3) and 1.971 (5) Å} are longer than the Co—N(imine) ones {1.885 (4) and 1.881 (4) Å} [39]. These values agree with values reported for similar cobalt(III) complexes [40]. Further, the C—S bond distances in both ligand anions are of 1.741 (6) Å and 1.744 (5) Å, indicating the TSC ligands in their thiol form [40]. In both ligands, the C—N and N—N bond lengths are intermediate between double- and single-bond characters owing to the delocalization of the charge along the entire ligand skeleton [39].

2.3. Bacterial Inhibition

Figure 8 shows the antibacterial assay results of **HL**¹, **HL**², **C1**, **C2** and the ampicillin drug (20 mg/mL in DMSO) against bacterial strains of *S. aureus* (Gram-positive) and *E. coli* (Gram-negative). The results are represented as the inhibition zone diameters (in mm) measured by the disc diffusion method of Kirby–Bauer [41]. Ampicillin afforded inhibitions with 21 and 25 mm against *S. aureus* and *E. coli*, respectively. The compounds **HL**¹, **HL**², **C1** and **C2** showed respectively inhibitions of 0, 10, 0 and 15 mm against *S. aureus* and of 0, 10, 0 and 12 mm against *E. coli*. These results indicate no activity of the ligand **HL**¹ and its respective complex against the studied bacterial strains. However, **HL**² and **C2** gave moderate antibacterial activities slightly higher for the complex against the two bacterial strains, but the activities are still less when compared with the standard. The inactivity of **HL**¹ and its complex, compared with the activities of **HL**² and **C2**, is probably due to their higher nitrogen content, as nitrogen is a vital element required for the growth of the microorganisms [42]. Indeed, metal complexes have been reported in several papers as long-acting drugs with slow releases in the cells, and the higher activities given by complexes relative to those of their ligands have been documented in several papers that concluded that upon coordination, the ligands bio-active or -inactive improved their antimicrobial activities or attained some pharmacological action [43,44].

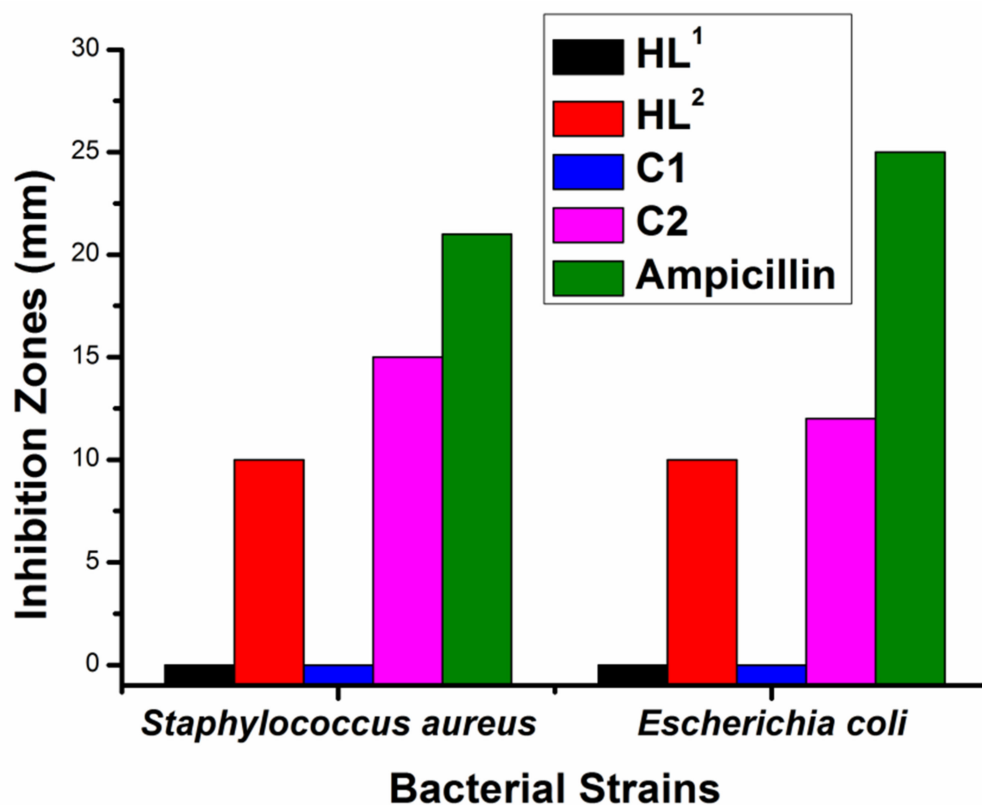


Figure 8. Correlation plot between the antibacterial activities against *S. aureus* and *E. coli*, expressed as the inhibition zone diameters in mm, and the compounds under investigation.

2.4. Cytotoxic Activity

To determine the anti-proliferative activity of the present TSC compounds, the cytotoxicity of ligand **HL**¹ against cells of A-549 human lung carcinoma, MCF-7 human breast cancer, HEPG-2 human liver cancer and HCT-116 human colon cancer was evaluated by the SRB assay method, which is more advantageous over the MTT method as the latter is more prone to interferences in the results not related to cell viability [45]. The ligand in five concentrations (0–100 µg/mL) was evaluated to determine the concentration against each cell, leading to 50% proliferation inhibition (IC₅₀ value). This preliminary test showed the greatest cytotoxic activity against MCF-7 cells (IC₅₀ = 15.8 µg/mL, cell proliferation = 9.6% at 100 µg/mL) and a bit less significant cytotoxic effect against HEPG-2 cells (IC₅₀ = 23.5 µg/mL, cell proliferation = 33.2% at 100 µg/mL). This is while the addition of up to 100 µg/mL of **HL**¹ offered cell proliferation of 64.1% and 60.4% in the A-549 and HCT-116 cancer cells, respectively.

Therefore, we compared the activities of all ligands and complexes against human epithelial-adenocarcinoma MCF-7 cells (model cells for breast cancer; the most prevalent cancer among women on the globe) [46]. Solutions of varied concentrations of all compounds (0–100 µg/mL) in DMSO were prepared, and the anti-proliferative activities against MCF-7 cells were found to follow a concentration-dependent manner (Figure 9). Indeed, the ligand **HL**² activity has much enhanced upon complexation, causing percent proliferation change from 47.7% by **HL**² to 38.7% by **C2** (compound concentration = 100 µg/mL), and IC₅₀ values of 145.4 and 49.9 µM were determined for the ligand and its complex, respectively. On the contrary, the ligand **HL**¹ showed great cytotoxic activity on this cell type and the complexation with cobalt inversely affected the ligand anti-proliferative activity; **HL**¹ and its complex at 100 µg/mL afforded cell proliferations of 9.6% (IC₅₀ = 52.4 µM) and 62.1%, respectively.

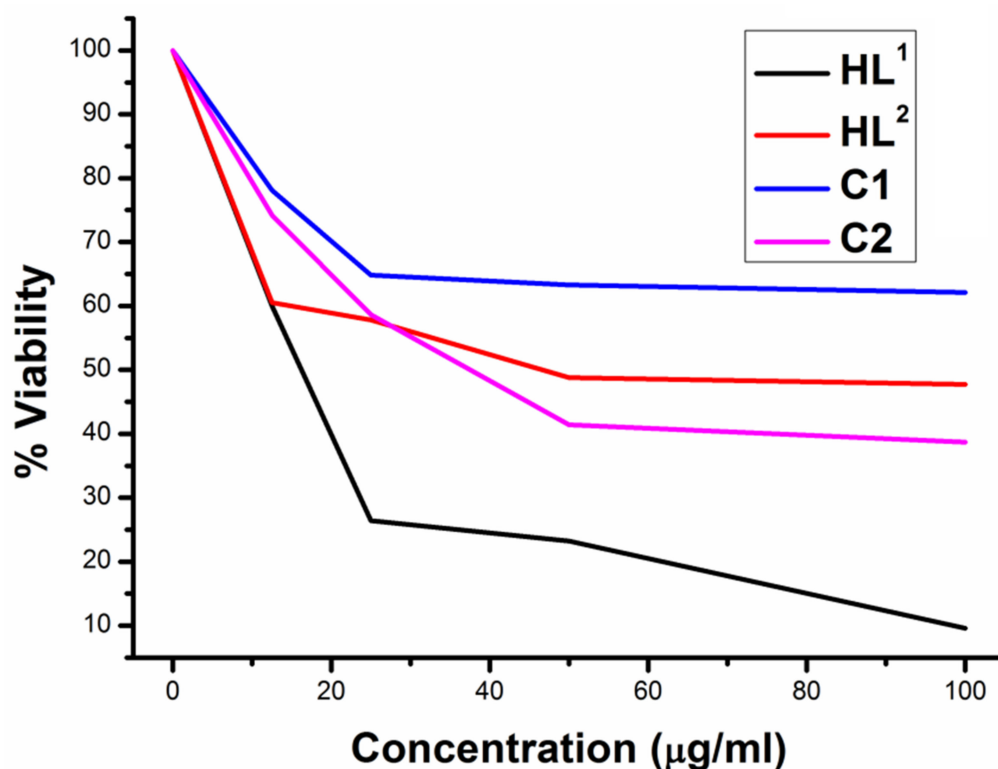


Figure 9. Anti-proliferative activities displayed by various concentrations of ligands (**HL**¹ and **HL**²) and complexes (**C1** and **C2**) against MCF-7 cancer breast cells.

These results (Table 3) {IC₅₀ of **HL**¹, **HL**² and **C2** = 52.4, 145.4 and 49.9 µM, respectively} in general indicate a high dependence on the substituents that the nitro group in ligand

HL¹ greatly enhanced through its anti-proliferative activity in comparison with that of **HL²**, while the much less activity of **C1** in comparison with that of **C2** is probably due to the more synergetic effect in **C2**. Indeed, three trivalent cobalt complexes with TSC ligands {4-(4-halophenyl)-1-((8-hydroxyquinoline-2-yl)methylene)thiosemicarbazones; halo = fluoro (HA), chloro (HB) and bromo (HC)} were reported in literature [46]. These complexes (ligands) exhibited anti-proliferative activities towards MCF-7 cells with IC₅₀ values of 195.9 (1111.5), 381.8 (1740.0) and 126.3 (1006.2) μM [47]. This means that the investigated compounds **HL¹**, **HL²** and **C2** in this paper, due to the redox activity of cobalt and structural diversity of the complexes, are exceptional [47]. Nevertheless, comparing these IC₅₀ values with the value of 9.66 μM given by doxorubicin as a standard drug under the same experimental conditions and with reported values for other standards {cisplatin (7.2 μM), carboplatin (0.02 μM) and tamoxifen (0.0455 μM)} [47] indicates lower activities by the TSC compounds under investigation.

Table 3. IC₅₀ values (μM) of MCF-7 cancer and BHK normal cells exposed to compounds **HL¹**, **HL²**, **C1**, **C2** and doxorubicin (dox).

	MCF-7					BHK				
	HL¹	HL²	C1	C2	dox	HL¹	HL²	C1	C2	dox
IC ₅₀ (μM)	52.4	145.4	>136.8 *	49.9	9.66	54.8	110.6	>136.8 *	>131.4 *	36.42

The cytotoxic activities of all compounds up to the concentration 100 μg/mL were determined. The IC₅₀ values marked with (*) were not investigated, because these values are greater than 100 μg/mL.

Finally, to fulfill this study, we measured the induced cytotoxicity by the TSC ligands, the cobalt complexes and doxorubicin to normal BHK (baby hamster kidney) cells. We determined an IC₅₀ value of 36.42 μM for doxorubicin and values of 54.8 and 110.6 μM for **HL¹** and **HL²**, respectively. However, interestingly, surviving fractions of normal BHK cells of 66.1% and 62.7% were determined, respectively, corresponding to concentration of 100 μg/mL of the complexes (136.8 μM of **C1** and 131.4 μM of **C2**), indicating a low toxicity to the normal BHK cells by the coordination compounds.

3. Materials and Methods

3.1. Materials and Physical Measurements

Hexahydrated cobalt chloride, 4-nitrophenyl isothiocyanate, 2,5-dimethoxyphenyl isothiocyanate, hydrazine hydrate, doxorubicin and pyridine-2-carboxaldehyde were purchased from reputable manufacturers (Alfa Aesar, Kandel, Germany; MERCK, Hohenbrunn, Germany or Sigma-Aldrich, Steinheim, Germany). All other chemicals were supplied in analytical-grade form and were used as they were received. All syntheses, manipulations, experiments and analyses were conducted in the air at ambient room temperature, unless mentioned otherwise. The TSC ligands, **HL¹** [28] and **HL²** [29], were each synthesized via two-step procedures following respective papers. The nuclear magnetic resonances (¹H NMR and ¹³C NMR) were provided in DMSO-d₆ with a Bruker 400 MHz spectrometer (Bruker Corporation, Billerica, MA, USA) equipped with TMS (i.e., tetramethylsilane) as an internal reference. Carbon, hydrogen, nitrogen and sulfur analyses were determined by the instrument Vario EL III CHNS Element Analyzer (elementar Analysensysteme GmbH, Langenselbold, Germany). Solution electrical-conductivities of complexes **C1** and **C2** (1 mM) in dimethylformamide were investigated by a Jenway 4320 conductivity meter (Cole-Parmer, Vernon Hills, IL, USA). All compounds' UV-visible absorption spectra were determined in CH₂Cl₂ with a Perkin-Elmer Lambda 40 UV/VIS spectrometer (PerkinElmer, Waltham, MA, USA), and the vibrational transitions in the compounds pressed in KBr pellets were scanned with the use of a Nicolet iS10 FT-IR spectrometer (Thermo Fisher Scientific, Waltham, MA, USA). Diamagnetism of the cobalt complexes was proven by a Sherwood MKI magnetic susceptibility balance (Sherwood Medical, St. Louis, Missouri, USA) utilizing Hg[Co(SCN)₄] as a calibration standard.

3.2. X-ray Crystallography

The crystallography studies on a single crystal of complex **C1** of dimensions $0.27 \times 0.16 \times 0.14$ mm were conducted at 123 (2) K using a Bruker D8 QUEST diffractometer (Bruker Corporation, Billerica, MA, USA) with MoK α radiation ($\lambda = 0.71073$ Å). The Bruker SAINT software package was used in the integration of the frames [48], and the multi-scan method (SADABS) for correcting the absorption effects [49]. The complex **C1** structure was solved with direct method and refined with SHELXTL program [50]. Anisotropic refinement for all non-H atoms was performed. The H-atoms were located at calculated positions by a riding model. The hydrogen atoms of the thiourea and hydrazine fragments were freely refined. The molecular graphic of complex **C1** was drawn with ORTEP-3 [51] with ellipsoid at 50% probability level.

3.3. Synthesis of the Complexes

A hundred milligrams of each TSC ligand (0.332 mmol of **HL**¹ or 0.316 mmol of **HL**²) was dissolved in warm methanol (10 mL), and CoCl₂·6H₂O (38–39 mg; 0.158–0.166 mmol) was added while stirring. The dark solutions were stirred for one hour at the room temperature, before standing in a fridge for a month. The complexes (single crystals of **C1** and microcrystals of **C2**) were filtered, washed with a few milliliters of methanol followed by diethyl ether and dried in the air.

[Co(L¹)₂]Cl₂H₂O **C1**: Yield = 81 mg (67%). Anal. Calcd.(Found) for C₂₆H₂₄N₁₀O₆S₂CoCl (MW = 731.05 g/mol), C = 42.72 (42.60) %, H = 3.31 (3.33) %, N = 19.16 (18.98) % and S = 8.77 (8.66) %. ¹H NMR (DMSO-d₆, ppm): 7.43 (1H, d, pyridine), 7.80 (1H, d, pyridine), 7.87 (1H, t, pyridine), 8.06 (1H, t, pyridine), 8.26 (2H, d, benzene), 8.40 (2H, d, benzene), 10.48 (1H, s, thiourea) and 12.19 (1H, s, azomethine). ¹³C NMR (DMSO-d₆, ppm): 125.25, 127.00, 145.75, 150.93 and 177.40. FT-IR (KBr, cm⁻¹) = 3312 ν (⁴NH), 1572 ν (C=N), 1312–791 [ν (CS) + ν (CN)], 1098 ν (N–N), 688 Py(iP), 589 ν (Co–N_{azomethine}) and 427 Py(OP). Electronic (dichloromethane, nm) = 239 and 384. Λ (DMF, Ω^{-1} cm²mol⁻¹) = 72.12. Magnetic moment = diamagnetic.

[Co(L²)₂]Cl₂H₂O **C2**: Yield = 71 mg (59%). Anal. Calcd.(Found) for C₃₀H₃₄N₈O₆S₂CoCl (MW = 761.16 g/mol), C = 47.34 (47.69) %, H = 4.50 (4.32) %, N = 14.72 (14.71) % and S = 8.43 (8.20) %. ¹H NMR (DMSO-d₆, ppm): 3.77 (3H, s, CH₃), 3.89 (3H, s, CH₃), 6.78 (1H, d, pyridine), 7.05 (2H, d, pyridine), 7.41 (1H, t, pyridine), 7.91 (1H, t, pyridine), 8.03 (1H, s, benzene), 8.13 (1H, d, benzene), 8.61 (1H, d, benzene), 10.10 (1H, s, thiourea) and 12.11 (1H, s, azomethine). ¹³C NMR (DMSO-d₆, ppm): 56.82, 58.32, 112.99, 120.57, 126.07, 137.99, 144.21 and 150.26. FT-IR (KBr, cm⁻¹) = 3394 ν (⁴NH), 1523 ν (C=N), 1314–819 [ν (CS) + ν (CN)], 1099 ν (N–N), 644 Py(iP), 578 ν (Co–N_{azomethine}) and 452 Py(OP). Electronic (dichloromethane, nm) = 255(sh), 296 and 428. Λ (DMF, Ω^{-1} cm²mol⁻¹) = 77.81. Magnetic moment = diamagnetic.

3.4. In Vitro Antibacterial Activity Assay

The antibacterial activity of the cobalt complexes, together with their respective ligands and ampicillin (reference drug) against *Staphylococcus aureus* ATCC 12600 G (+ve) and *Escherichia coli* ATCC 11775 G (–ve) bacteria received from the American Tissue Culture Collection (ATCC, Alexandria, MN, USA), was assayed in triplicate via the modified Kirby–Bauer disc diffusion method [41]. From each bacterium, a volume of 100 μ L was moved to nutrient broth medium (10 mL) and allowed to reach the count of 5×10^8 cells/mL. From each bacterial culture, a suspension of 100 μ L was taken and layered on agars containing fresh media. The bacterial species were incubated for 1 day at 37 °C. A solution (20 mg/mL) in DMSO of each compound that its antibacterial effect was to be investigated was prepared, and 8.0 mm blank paper discs (Schleicher & Schuell, Sevilla, Spain) were each impregnated with a volume of ten microliters from each solution. The placement of these discs onto the bacterial agars caused the diffusion of the compound solution and the inhibition of the bacterial growth around the discs. The inhibition zones were determined with slipping callipers according to the National Committee for Clinical Laboratory Standards.

3.5. Cytotoxic Activity against Cancer and Normal Cell Lines

Human cancer cells of lungs (A-549), breasts (MCF-7), livers (HEPG-2) and colons (HCT-116) and normal cells of baby hamster kidneys (BHKs) were originally received from the American Tissue Culture Collection (ATCC, Alexandria, MN, USA) and kept at the National Cancer Institute in Cairo (Egypt) by serial sub-culturing. The activities given by the TSCs were investigated in triplicate according to a published paper [45]. First, the incubation of the cells (4000 cells/well) into 96-well microtiter tissue culture microplates was performed in fresh medium (200 μ L) at 37 °C and less than 5% of CO₂. One day afterwards, all compounds, including doxorubicin as a reference drug, were freshly dissolved in DMSO to form a series of 0–100 μ g/mL solutions of each compound, and each solution was added to a cell plate. Incubation was conducted further for 48 h, and the cultures were fixed by layering cold trichloroacetic acid (50%, 50 μ L) at 4 °C on each well. The cell cultures were washed with distilled water, before staining with fifty microliters of sulphorhodamine B (SRB, 0.4%) solution in acetic acid (1%) for half an hour in the dark at ambient atmosphere. After rewashing with acetic acid (1%) and air drying, TRIS (10 mM, pH 10.5, 200 μ L) was added to each well to solubilize the dye. The optical density of each well was investigated at 570 nm by employing an ELISA microtiter plate reader.

4. Conclusions

In this paper, two cobalt complexes (**C1** and **C2**) derived from tridentate thiosemi-carbazones of pyridine-2-carboxyldehyde (**HL**¹ and **HL**²) were prepared. The analysis revealed the 1:1 ionic nature and trivalent oxidation state of cobalt in the complexes. XRD studies indicated full structural parameters in complex **C1**. Antibacterial and anticancer activities of the ligands and complexes were investigated. Most pronounced, complexation with cobalt in complex **C2** enhanced the antibacterial activity of the ligand against *S. aureus* and *E. coli*, but the activities are still less compared with the induced activities by the ampicillin standard. However, against human MCF-7 cancer cells, both **HL**¹ and complex **C2** afforded good results, greater than the results given by several Co-TSC complexes, but lower than the activity given by doxorubicin. Nevertheless, doxorubicin induced higher cytotoxicity towards BHK normal cells compared with the ligands, and the toxicities towards normal BHK cells by the complexes were much lower.

Author Contributions: Conceptualization, A.B.M.I., S.A.E. and S.M.A.; methodology, A.F., A.B.M.I., A.V. and S.M.A.; crystal structure analysis, A.V.; investigation, A.F., A.B.M.I. and S.M.A.; writing—original draft preparation, A.B.M.I.; writing—review and editing, A.F., A.B.M.I., S.A.E., A.V. and S.M.A.; visualization, A.B.M.I. and A.V.; supervision, A.B.M.I., S.A.E. and S.M.A. All authors have read and agreed to the published version of the manuscript.

Funding: This research received no external funding.

Data Availability Statement: Crystallographic data for complex **C1** have been deposited with the Cambridge Crystallographic Data Centre, CCDC, 12 Union Road, Cambridge CB21EZ, UK. Copies of the data can be obtained free of charge on quoting the depository number CCDC-2175750 (<https://www.ccdc.cam.ac.uk/structures/> (accessed on 1 July 2022)).

Conflicts of Interest: The authors declare no conflict of interest.

References

1. Brown, K.L. Chemistry and Enzymology of Vitamin B12. *Chem. Rev.* **2005**, *105*, 2075–2150. [[CrossRef](#)] [[PubMed](#)]
2. Thorarinsdottir, A.E.; Du, K.; Collins, J.H.P.; Harris, T.D. Ratiometric pH Imaging with a CoII2 MRI Probe via CEST Effects of Opposing pH Dependences. *J. Am. Chem. Soc.* **2017**, *139*, 15836–15847. [[CrossRef](#)] [[PubMed](#)]
3. Kim, B.J.; Hambley, T.W.; Bryce, N.S. Visualising the hypoxia selectivity of cobalt(III) prodrugs. *Chem. Sci.* **2011**, *2*, 2135–2142. [[CrossRef](#)]
4. Hurtado, R.R.; Harney, A.S.; Heffern, M.C.; Holbrook, R.J.; Holmgren, R.A.; Meade, T.J. Specific Inhibition of the Transcription Factor Ci by a Cobalt(III) Schiff Base–DNA Conjugate. *Mol. Pharm.* **2012**, *9*, 325–333. [[CrossRef](#)]

5. Renfrew, A.K.; Bryce, N.S.; Hambley, T. Cobalt(III) Chaperone Complexes of Curcumin: Photoreduction, Cellular Accumulation and Light-Selective Toxicity towards Tumour Cells. *Chem. Eur. J.* **2015**, *21*, 15224–15234. [[CrossRef](#)]
6. Cressey, P.B.; Eskandari, A.; Bruno, P.M.; Lu, C.; Hemann, M.T.; Suntharalingam, K. The Potent Inhibitory Effect of a Naproxen-Appended Cobalt(III)-Cyclam Complex on Cancer Stem Cells. *ChemBioChem* **2016**, *17*, 1713–1718. [[CrossRef](#)]
7. Schwartz, J.A.; Lium, E.K.; Silverstein, S.J. Herpes Simplex Virus Type 1 Entry Is Inhibited by the Cobalt Chelate Complex CTC-96. *J. Virol.* **2001**, *75*, 4117–4128. [[CrossRef](#)]
8. Weiqun, Z.; Wen, Y.; Liqun, X.; Xianchen, C. N-Benzoyl-N'-dialkylthiourea derivatives and their Co(III) complexes: Structure, and antifungal. *J. Inorg. Biochem.* **2005**, *99*, 1314–1319. [[CrossRef](#)]
9. Miodragovic, D.U.; Bogdanovic, G.A.; Miodragovic, Z.M.; Radulovic, M.D.; Novakovic, S.B.; Kaludjerovic, G.N.; Kozlowski, H. Interesting coordination abilities of antiulcer drug famotidine and antimicrobial activity of drug and its cobalt(III) complex. *J. Inorg. Biochem.* **2006**, *100*, 1568–1574. [[CrossRef](#)]
10. Wegner, S.V.; Spatz, J.P. Cobalt(III) as a Stable and Inert Mediator Ion between NTA and His6-Tagged Proteins. *Angew. Chem. Int. Ed.* **2013**, *52*, 7593–7596. [[CrossRef](#)]
11. Hall, M.D.; Failes, T.W.; Yamamoto, N.; Hambley, T.W. Bioreductive activation and drug chaperoning in cobalt pharmaceuticals. *Dalton Trans.* **2007**, 3983–3990. [[CrossRef](#)]
12. Finch, R.A.; Liu, M.C.; Grill, S.P.; Rose, W.C.; Loomis, R.; Vasquez, K.M.; Cheng, Y.C.; Sartorelli, A.C. Triapine (3-aminopyridine-2-carboxaldehyde-thiosemicarbazone): A potent inhibitor of ribonucleotide reductase activity with broad spectrum antitumor activity. *Biochem. Pharmacol.* **2000**, *59*, 983–991. [[CrossRef](#)]
13. Gojo, I.; Tidwell, M.L.; Greer, J.; Takebe, N.; Seiter, K.; Pochron, M.F.; Johnson, B.; Sznol, M.; Karp, J.E. Phase I and pharmacokinetic study of Triapine[®], a potent ribonucleotide reductase inhibitor, in adults with advanced hematologic malignancies. *Leuk. Res.* **2007**, *31*, 1165–1173. [[CrossRef](#)]
14. Wadler, S.; Makower, D.; Clairmont, C.; Lambert, P.; Fehn, K.; Sznol, M. Phase I and Pharmacokinetic Study of the Ribonucleotide Reductase Inhibitor, 3-Aminopyridine-2-Carboxaldehyde Thiosemicarbazone, Administered by 96-Hour Intravenous Continuous Infusion. *J. Clin. Oncol.* **2004**, *22*, 1553–1563. [[CrossRef](#)]
15. Karp, J.E.; Giles, F.J.; Gojo, I.; Morris, L.; Greer, J.; Johnson, B.; Thein, M.; Sznol, M.; Low, J. A Phase I study of the novel ribonucleotide reductase inhibitor 3-aminopyridine-2-carboxaldehyde thiosemicarbazone (3-AP, Triapine[®]) in combination with the nucleoside analog fludarabine for patients with refractory acute leukemias and aggressive myeloproliferative disorders. *Leuk. Res.* **2008**, *32*, 71–77.
16. Allen, F.H. The Cambridge Structural Database: A quarter of a million crystal structures and rising. *Acta Crystallogr. B* **2002**, *58*, 380–388. [[CrossRef](#)]
17. El-Ayaan, U.; Youssef, M.M.; Al-Shihry, S. Mn(II), Co(II), Zn(II), Fe(III) and U (VI) complexes of 2-acetylpyridine 4N-(2-pyridyl) thiosemicarbazone (HAPT); structural, spectroscopic and biological studies. *J. Mol. Struct.* **2009**, *936*, 213–219. [[CrossRef](#)]
18. Sampath, K.; Sathiyaraj, S.; Jayabalakrishnan, C. DNA binding, DNA cleavage, antioxidant and cytotoxicity studies on ruthenium(II) complexes of benzaldehyde 4-methyl-3-thiosemicarbazones. *Spectrochim. Acta A* **2013**, *105*, 582–592. [[CrossRef](#)]
19. Reis, D.C.; Pinto, M.C.X.; Souza-Fagundes, E.M.; Wardell, S.M.S.V.; Wardell, J.L.; Beraldo, H. Antimony(III) complexes with 2-benzoylpyridine-derived thiosemicarbazones: Cytotoxicity against human leukemia cell lines. *Eur. J. Med. Chem.* **2010**, *45*, 3904–3910. [[CrossRef](#)]
20. Pathan, A.H.; Ramesh, A.K.; Bakale, R.P.; Naik, G.N.; Kumar, H.G.R.; Frampton, C.S.; Rao, G.M.A.; Gudasi, K.B. Association of late transition metal complexes with ethyl 2-(2-(4-chlorophenylcarbamothioyl)hydrazono)propanoate: Design, synthesis and in vitro anticancer studies. *Inorg. Chim. Acta* **2015**, *430*, 216–224. [[CrossRef](#)]
21. Mendes, I.C.; Soares, M.A.; Dos Santos, R.G.; Pinheiro, C.; Beraldo, H. Gallium(III) complexes of 2-pyridineformamide thiosemicarbazones: Cytotoxic activity against malignant glioblastoma. *Eur. J. Med. Chem.* **2009**, *44*, 1870–1877. [[CrossRef](#)]
22. Da Silva, J.G.; Azzolini, L.S.; Wardell, S.M.S.V.; Wardell, J.L.; Beraldo, H. Increasing the antibacterial activity of gallium(III) against *Pseudomonas aeruginosa* upon coordination to pyridine-derived thiosemicarbazones. *Polyhedron* **2009**, *28*, 2301–2305. [[CrossRef](#)]
23. Mendes, I.C.; Moreira, J.P.; Ardisson, J.D.; Dos Santos, R.G.; Da Silva, P.R.O.; Garcia, I.; Castiñeiras, A.; Beraldo, H. Organotin(IV) complexes of 2-pyridineformamide-derived thiosemicarbazones: Antimicrobial and cytotoxic effects. *Eur. J. Med. Chem.* **2008**, *43*, 1454–1461. [[CrossRef](#)]
24. Parrilha, G.L.; Da Silva, J.G.; Gouveia, L.F.; Gasparoto, A.K.; Dias, R.P.; Rocha, W.R.; Santos, D.A.; Speziali, N.L.; Beraldo, H. Pyridine-derived thiosemicarbazones and their tin(IV) complexes with antifungal activity against *Candida* spp. *Eur. J. Med. Chem.* **2011**, *46*, 1473–1482. [[CrossRef](#)]
25. Merlino, A.; Benitez, D.; Chavez, S.; Da Cunha, J.; Hernandez, P.; Tinoco, L.W.; Campillo, N.E.; Paez, J.A.; Cerecetto, H.; Gonzalez, M. Development of second generation amidinohydrazones, thio- and semicarbazones as *Trypanosoma cruzi*-inhibitors bearing benzofuroxan and benzimidazole 1,3-dioxide core scaffolds. *Med. Chem. Commun.* **2010**, *1*, 216–228. [[CrossRef](#)]
26. Parrilha, G.L.; Dias, R.P.; Rocha, W.R.; Mendes, I.C.; Benitez, D.; Varela, J.; Cerecetto, H.; Gonzalez, M.; Melo, C.M.L.; Neves, J.K.A.L.; et al. 2-Acetylpyridine- and 2-benzoylpyridine-derived thiosemicarbazones and their antimony(III) complexes exhibit high anti-trypanosomal activity. *Polyhedron* **2012**, *31*, 614621. [[CrossRef](#)]
27. Klayman, D.L.; Bartosevich, J.F.; Griffin, T.S.; Mason, C.J.; Scovill, J.P. 2-Acetylpyridine thiosemicarbazones. 1. A new class of potential antimalarial agents. *J. Med. Chem.* **1979**, *22*, 855–862. [[CrossRef](#)]

28. Pape, V.F.S.; Tóth, S.; Füred, A.; Szebényi, K.; Lovrics, A.; Szabó, P.; Wiese, M.; Szakács, G. Design, synthesis and biological evaluation of thiosemicarbazones, hydrazinobenzothiazoles and arylhydrazones as anticancer agents with a potential to overcome multidrug resistance. *Eur. J. Med. Chem.* **2016**, *117*, 335–354. [[CrossRef](#)]
29. Ibrahim, A.B.M.; Farh, M.K.; Mayer, P. Copper complexes of new thiosemicarbazone ligands: Synthesis, structural studies and antimicrobial activity. *Inorg. Chem. Commun.* **2018**, *94*, 127–132. [[CrossRef](#)]
30. Ibrahim, A.B.M.; Farh, M.K.; Plaisier, J.R.; Shalaby, E.M. Synthesis, structural and antimicrobial studies of binary and ternary complexes of a new tridentate thiosemicarbazone. *Future Med. Chem.* **2018**, *10*, 2507–2519. [[CrossRef](#)]
31. Ibrahim, A.B.M.; Farh, M.K.; Mayer, P. Synthesis, structural studies and antimicrobial evaluation of nickel (II) complexes of NNS tridentate thiosemicarbazone based ligands. *Appl. Organomet. Chem.* **2019**, *33*, e4883. [[CrossRef](#)]
32. Ibrahim, A.B.M.; Farh, M.K.; Santos, I.C.; Paulo, A. Nickel Complexes Bearing SNN and SS Donor Atom Ligands: Synthesis, Structural Characterization and Biological activity. *Appl. Organomet. Chem.* **2019**, *33*, e5088. [[CrossRef](#)]
33. Ibrahim, A.B.M.; Farh, M.K.; El-Gyar, S.A.; EL-Gahami, M.A.; Fouad, D.M.; Silva, F.; Santos, I.C.; Paulo, A. Synthesis, structural studies and antimicrobial activities of manganese, nickel and copper complexes of two new tridentate 2-formylpyridine thiosemicarbazone ligands. *Inorg. Chem. Commun.* **2018**, *96*, 194–201. [[CrossRef](#)]
34. Mahmoud, G.A.-E.; Ibrahim, A.B.M.; Mayer, P. Zn(II) and Cd(II) thiosemicarbazones for stimulation/inhibition of kojic acid biosynthesis from *Aspergillus flavus* and the fungal defense behavior against the metal complexes' excesses. *J. Biol. Inorg. Chem.* **2020**, *25*, 797–809. [[CrossRef](#)] [[PubMed](#)]
35. Geary, W.J. The use of conductivity measurements in organic solvents for the characterization of coordination compounds. *Coord. Chem. Rev.* **1971**, *7*, 81–122. [[CrossRef](#)]
36. Filipović, N.R.; Bjelogrić, S.; Portalone, G.; Pelliccia, S.; Silvestri, R.; Klisurić, O.; Senčanski, M.; Stanković, D.; Todorović, T.R.; Muller, C.D. Pro-apoptotic and pro-differentiation induction by 8-quinolinecarboxaldehyde selenosemicarbazone and its Co(III) complex in human cancer cell lines. *Med. Chem. Commun.* **2016**, *7*, 1604–1616. [[CrossRef](#)]
37. Giriraj, K.; Kasim, M.S.M.; Balasubramaniam, K.; Thangavel, S.K.; Venkatesan, J.; Suresh, S.; Shanmugam, P.; Karri, C. Various coordination modes of new coumarin Schiff bases toward Cobalt (III) ion: Synthesis, spectral characterization, in vitro cytotoxic activity, and investigation of apoptosis. *Appl. Organomet. Chem.* **2022**, *36*, e6536. [[CrossRef](#)]
38. West, D.X.; Swearingena, J.K.; Martinez, J.V.; Ortega, S.H.; El-Sawaf, A.K.; Meursd, F.; Castineirase, A.; Garciae, I.; Bermejoe, E. Spectral and structural studies of iron(III), cobalt(II,III) and nickel(II) complexes of 2-pyridineformamide N(4)-methylthiosemicarbazone. *Polyhedron* **1999**, *18*, 2919–2929. [[CrossRef](#)]
39. Manikandan, R.; Viswanathamurthi, P.; Velmurugan, K.; Nandhakumar, R.; Hashimoto, T.; Endo, A. Synthesis, characterization and crystal structure of cobalt(III) complexes containing 2-acetylpyridine thiosemicarbazones: DNA/protein interaction, radical scavenging and cytotoxic activities. *J. Photochem. Photobiol. B Biol.* **2014**, *130*, 205–216. [[CrossRef](#)]
40. Saha, N.C.; Saha, N.; Chaudhuri, S. X-ray structures of cobalt(III) complexes with bio-relevant pyrazolyl thiosemicarbazone: Indication of structural changes on the increasing bulkiness of the alkyl substituents on thiosemicarbazone moiety. *Struct. Chem.* **2007**, *18*, 245–251. [[CrossRef](#)]
41. Fekete, T.; Tumah, H.; Woodwell, J.; Truant, A.; Satischandran, V.; Axelrod, P.; Kreter, B. A comparison of serial plate agar dilution, bauer-kirby disk diffusion, and the vitek automicrobic system for the determination of susceptibilities of *Klebsiella* spp., *Enterobacter* spp., and *Pseudomonas aeruginosa* to ten antimicrobial agents. *Diagn. Microbiol. Infect. Dis.* **1994**, *18*, 251–258. [[CrossRef](#)]
42. Ibrahim, A.B.M.; Mahmoud, G.A.-E.; Cordes, D.B.; Slawin, A.M.Z. Pb (II) and Hg (II) thiosemicarbazones for inhibiting the broad-spectrum pathogen *Cladosporium sphaerospermum* ASU18 (MK387875) and altering its antioxidant system. *Appl. Organomet. Chem.* **2022**, *36*, e6798. [[CrossRef](#)]
43. Abdolmaleki, S.; Yarmohammadi, N.; Adibi, H.; Ghadermazi, M.; Ashengroph, M.; Rudbari, H.A.; Bruno, G. Synthesis, X-ray studies, electrochemical properties, evaluation as in vitro cytotoxic and antibacterial agents of two antimony (III) complexes with dipicolinic acid. *Polyhedron* **2019**, *159*, 239–250. [[CrossRef](#)]
44. Ferraz, K.S.O.; Silva, N.F.; da Silva, J.G.; de Miranda, L.F.; Romeiro, C.F.D.; Souza-Fagundes, E.M.; Mendes, I.C.; Beraldo, H. Investigation on the pharmacological profile of 2,6-diacetylpyridine bis(benzoylhydrazone) derivatives and their antimony(III) and bismuth(III) complexes. *Eur. J. Med. Chem.* **2012**, *53*, 98–106. [[CrossRef](#)]
45. Skehan, P.; Storeng, R.; Scudiero, D.; Monks, A.; McMahon, J.; Vistica, D.; Warren, J.T.; Bokesch, H.; Kenney, S.; Boyd, M.R. New Colorimetric Cytotoxicity Assay for Anticancer-Drug Screening. *J. Natl. Cancer Inst.* **1990**, *82*, 1107–1112. [[CrossRef](#)]
46. Kotian, A.; Kamat, V.; Naik, K.; Kokare, D.G.; Kumara, K.; Neratur, K.L.; Kumbar, V.; Bhat, K.; Revankar, V.K. 8-Hydroxyquinoline derived p-halo N4-phenyl substituted thiosemicarbazones: Crystal structures, spectral characterization and in vitro cytotoxic studies of their Co(III), Ni(II) and Cu(II) complexes. *Bioorg. Chem.* **2021**, *112*, 104962. [[CrossRef](#)]
47. Hadjikakou, S.K.; Ozturk, I.I.; Banti, C.N.; Kourkoumelis, N.; Hadjiliadis, N. Recent advances on antimony(III/V) compounds with potential activity against tumor cells. *J. Inorg. Biochem.* **2015**, *153*, 293–305. [[CrossRef](#)]
48. The program BrukerSAINT, Bruker AXS Inc.: Madison, WI, USA, 2012.
49. Sheldrick, G.M. *SADABS Software for Empirical Absorption Corrections*; University of Göttingen: Göttingen, Germany, 1996.
50. Sheldrick, G.M. SHELXT—Integrated space-group and crystal-structure determination. *Acta Cryst.* **2015**, *A71*, 3–8. [[CrossRef](#)]
51. Farrugia, L.J. WinGX and ORTEP for Windows: An update. *J. Appl. Crystallogr.* **2012**, *45*, 849–854. [[CrossRef](#)]